The conserved 5′ apical hairpin stem loops of bamboo mosaic virus and its satellite RNA contribute to replication competence

Hsin-Chuan Chen[1], Lih-Ren Kong[1], Ting-Yu Yeh[1], Chi-Ping Cheng[1], Yau-Heiu Hsu[2] and Na-Sheng Lin[1,*]

[1]Institute of Plant and Microbial Biology, Academia Sinica, Taipei and [2]Graduate Institute of Biotechnology, National Chung Hsing University, Taichung, Taiwan

ABSTRACT

Satellite RNAs associated with *Bamboo mosaic virus* (satBaMVs) depend on BaMV for replication and encapsidation. Certain satBaMVs isolated from natural fields significantly interfere with BaMV replication. The 5′ apical hairpin stem loop (AHSL) of satBaMV is the major determinant in interference with BaMV replication. In this study, by *in vivo* competition assay, we revealed that the sequence and structure of AHSL, along with specific nucleotides (C^{60} and C^{83}) required for interference with BaMV replication, are also involved in replication competition among satBaMV variants. Moreover, all of the 5′ ends of natural BaMV isolates contain the similar AHSLs having conserved nucleotides (C^{64} and C^{86}) with those of interfering satBaMVs, suggesting their co-evolution. Mutational analyses revealed that C^{86} was essential for BaMV replication, and that replacement of C^{64} with U reduced replication efficiency. The non-interfering satBaMV interfered with BaMV replication with the BaMV-C64U mutant as helper. These findings suggest that two cytosines at the equivalent positions in the AHSLs of BaMV and satBaMV play a crucial role in replication competence. The downregulation level, which is dependent upon the molar ratio of interfering satBaMV to BaMV, implies that there is competition for limited replication machinery.

INTRODUCTION

The genomes of positive-strand RNA viruses contain multiple functional RNA elements (1) that are responsible for performing specific tasks in a variety of fundamental viral processes including the synthesis of viral RNA (2,3), translation of the viral gene (4), cell-to-cell movement (5) and formation of the viral particle (6–8). Satellite RNAs (satRNAs) are subviral agents that depend on their cognate helper viruses for replication, movement and encapsidation. Since there are little or no significant sequence similarities between satRNAs and helper viruses (9–11), the RNA elements required for satRNA replication are distinct from those of the helper. However, increasing evidence has shown that satRNAs contain specific *cis*-sequences and/or structure adaptations that recognize the RNA-dependent RNA polymerase (RdRp) of the helper virus, thus enabling replication (12,13). For example, the conserved 5′ terminal T-shaped domain and down stream domain found in different tombusvirus genomes and satRNAs are involved in viral RNA replication (14,15); the 3′ terminus of *Cucumber mosaic virus* (CMV) satellite RNA shares considerable sequence and structural similarity with the tRNA-like structure of CMV genomic RNAs (16); and mimicry of the 5′- and 3′ termini was found in *Bamboo mosaic virus* (BaMV) and its associated satellite RNA (satBaMV) (17–19). These and other satRNAs have evolved various elements or structures to mimic their helper viruses in order to use the resources provided by these helpers (12).

Similar to RNA viruses, satRNAs contain great genetic heterogeneity as a result of error-prone replication of RNA genomes (20). The replication of satRNA could enhance, attenuate or not affect the pathogenicity of the helper virus depending on the propagation host, the helper virus and the satRNA variant (21). Some domains in satRNAs have also been found to be responsible for pathogenic phenotypes. For example, the region near the 5′ end of the satRNA variant NM3c involved in this variant's replication is also required for downregulation of

Groundnut rosette virus (GRV) replication and attenuation of GRV-induced symptoms (22); the necrogenicity domain of CMV satRNAs is a hairpin structure containing an octanucleotide loop and an adjacent stem within the 5′ half of the minus-strand that induces necrosis in tomato plants (23). Moreover, domains of satRNA variants involved in the pathogenic phenotypes might also be involved in their replication competition. For example, tomato plants co-inoculated with CMV-77.2 and mixtures of two satRNA variants, Tfn-satRNA (a benign variant) and 77-satRNA (a necrogenic variant), showed necrosis symptoms and the selective accumulation of 77-satRNA (24); satRNA B10, which attenuates the symptoms induced by TBSV, was the dominant species when co-inoculated with non-interfering satRNA B1 under the help of TBSV-Ch (25). Whether the necrosis domain of CMV satRNA is involved in the replication competition among satRNA variants is still unknown. The domain of satRNA B10 required for attenuating TBSV-induced symptoms also remains to be determined.

BaMV belongs to the potexvirus genus and has a single-stranded, positive-sense RNA genome of ∼6400 nt. The genomic RNA of BaMV contains five conserved open reading frames (ORFs) flanked by 5′- and 3′-untranslated regions (UTRs) of 94 and 142 nt, respectively (Figure 1A) (26,27). ORF 1 encodes a 155-kDa viral replicase containing capping enzyme (28–30), helicase (31) and RdRp domains (32). ORFs 2–4 encode triple block proteins of 28, 13 and 6 kDa, respectively, which are involved in cell-to-cell movement of the virus (33,34). ORF 5 encodes the 25-kDa capsid protein, which is required for viral RNA encapsidation, movement and symptom expression (35). Some BaMV isolates also contain satBaMV, which is a linear RNA molecule of 836 nt with a single ORF for a 20-kDa protein flanked by a 5′-UTR of 159 nt and a 3′-UTR of 125 nt (36). Recent studies revealed several common functional RNA elements and structures in the 5′- and 3′-UTRs of BaMV and satBaMV (12,19). In the 5′-UTR, the GAAA(A) repeats in the very termini and conserved secondary structure of the apical hairpin stem loop (AHSL) of BaMV and satBaMV play crucial roles in BaMV and satBaMV replication (Figure 1B) (18,37). Similarly, highly conserved hexanucleotides (ACCUAA) shared among potexvirus members, which are critical for recognition by the viral replicase (38,39), and polyadenylation signals (AAUAA A) were found in the 3′-UTR of BaMV and satBaMV. The 3′-UTRs of BaMV and satBaMV fold into a common BCD domain engaged in viral and satRNA replication, except for the lack of stem loop A (A domain) and a pseudoknot (E domain) in the 3′-UTR of satBaMV (Figure 1C) (19,40,41). Domains of B–E are involved in BaMV replication, whereas domain A is dispensable for replication but signifies a role in the long distance movement of BaMV (42,43). The 3′-UTR of satBaMV is non-interchangeable with BaMV 3′-UTR (19).

Natural satBaMV isolates from 11 infected bamboo species can be categorized into two major phylogenetic groups (44,45). Regardless of the phylogenetic group, some interfering satBaMVs have been found to be associated with natural BaMV infection. The well-studied one, BSL6, remarkably reduces the accumulation of BaMV RNA and attenuates BaMV-induced symptoms in co-inoculated plants, whereas the non-interfering satBaMV, BSF4, does not (46). The 5′-UTR of BSL6 has been shown to be responsible for downregulation of BaMV replication (47). The secondary structure of BSL6 5′-UTR contains one long stem-loop (LSL) and four small stem-loops (SSLs) (Figure 1B) (17), whereas the 5′-UTR of BSF4 folds into one LSL and a SSL (Figure 1B) (48). Strikingly, most of the hypervariable (HV) region, with divergence of up to 20%, in the 5′-UTRs of satBaMV variants fold into a conserved AHSL (45). The AHSL comprises an apical loop followed by two internal loops (IL-I and IL-II) interwoven by 3- to 4-, 2- and 5 base-paired stems located at the top of the LSL (Figure 1B), and this region is indispensable for the replication of satBaMV (17,45,47,48). This region is also the key determinant of interfering satBaMV to mediate downregulation of BaMV replication (47). The maintenance of both the secondary structure and the specific nucleotides of the AHSL are required for satBaMV-mediated interference of BaMV replication (17).

In this study, we performed *in vivo* competition assay by examining the progeny population in *Nicotiana benthamiana* co-infected with a mixture of interfering and non-interfering satBaMVs. We found that the interfering satBaMV was the dominant species. The RNA structure and nucleotide sequence required for this dominance were determined to be within the AHSL region, and were also conserved in all natural BaMV isolates. Our results show that the conserved 5′ AHSLs of BaMV and satBaMV play a crucial role in replication competence.

MATERIALS AND METHODS

Plasmid construction

Plasmid pBSF4 and pBSL6 are full-length cDNA clones of satBaMVs with a T7 RNA promoter at the 5′ end (46,49). SatBaMV mutants pBSF4-1 and pBSF4-5 derived from pBSF4 and mutants pBSL6-1 and pBSL6-11 derived from pBSL6 were described previously (17,47). Plasmid pBaMV is a full-length cDNA clone of BaMV-S with a T7 RNA promoter at the 5′ end (50). Plasmid pCB is a full-length cDNA clone of BaMV-S with a double 35S promoter from *Cauliflower mosaic virus* at the 5′ terminus in the pCass2 vector (51); plasmid pCBSF4 is a full-length cDNA clone of satBaMV BSF4 in the same vector (51). Plasmid pBaORF1 with a full-length cDNA of BaMV-S ORF1 and plasmid pBaORF1dGDD with the GDD motif deleted in BaMV-S ORF1 are also cloned in the pCass2 vector (52). To generate pCBSL6, a PCR fragment was synthesized from a pBSL6 template with the primers BS104 (5′-GAAAACTCACCGCAACGA) and BS99 [5′-CGGAATTCT$_{(15)}$]. The PCR product was further cleaved with *Eco*RI and phosphorylated by T4 polynucleotide kinase, then ligated into a *Stu*I/*Eco*RI-digested pCass2 vector. For construction of pCBSF4-1,
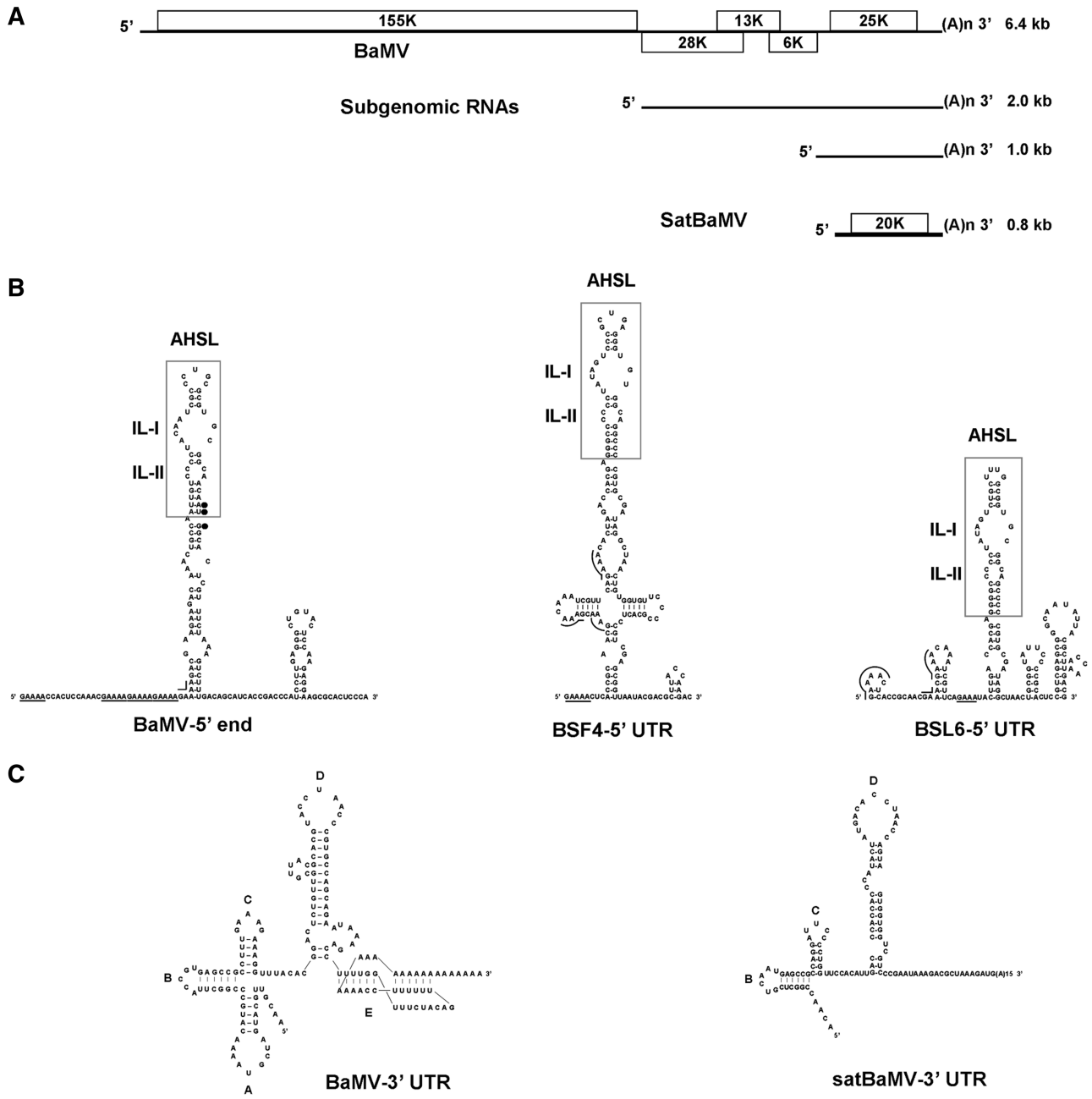
Figure 1. Genetic maps and 5′ and 3′-UTR secondary structures of BaMV and satBaMVs. (**A**) Genome organization and ORFs of BaMV and satBaMV. ORFs and the molecular weight of encoded proteins are shown in boxes. Two subgenomic RNAs of BaMV are presented by lines. (**B**) The secondary structures of the 5′-UTRs of BaMV and satBaMVs. The AHSL structures of BaMV and satBaMV are boxed, and contain an apical loop and two internal loops (IL-1 and IL-2). Black circles indicate the start codon of BaMV ORF1. The common GAAA(A) repeats in the 5′-UTRs of BaMV and satBaMV are underlined. (**C**) The secondary structure of the BaMV 3′-UTR contains a cloverleaf-like ABC domain, a stem loop D (D domain) and a pseudoknot (E domain) (40,41). The secondary structure of the satBaMV 3′-UTR is similar to that of BaMV except for the lack of A and E domains (19).

a PCR fragment was synthesized from a pBSF4-1 template with the primers Sat-F (5′-GGTACCGAAAAC TCACCGCAACGAAAC) and SatF4-1-R (GAATTCAT CTTTTAGCGTCTTTATTCGG). The PCR product was further cleaved with *Kpn*I and *Eco*RI, and ligated into a *Kpn*I/*Eco*RI-digested pCass2 vector. Plasmid pCBSL6-1 was constructed in the same way except that the template and reverse primer using in the PCR were

pBSL6-1 and SatL6-1-R (GAATTCATCTTTTAACGT CTTTATTCGG), respectively. The mutant pBaMV-C86U was constructed by site-directed mutagenesis using a double-PCR method (48) in which an ~100-bp fragment of BaMV 5′ end was amplified from the pBaMV template by the primer pair B162 [5′-GCTCTAGAGTAATACG ACTCACTATAGAAAAG(C)CAT(C)TCCAAACA(G)-3′] and C86U-R (5′-ATTGTTGCCACACGCGCAGG-3′)

using *Pfu* DNA polymerase (Promega, WI, USA). This fragment was purified and mixed with a reverse primer, B80 (5′-AGCTTGGCCCAAACATC-3′), to amplify an ~1-kb fragment of the BaMV-C86U mutant. The PCR product was further cleaved with *Bam*HI and *Xba*I and ligated into a *Bam*HI/*Xba*I-digested pBaMV vector. The mutant pBaMV-C64U was constructed by the same way except that the reverse primer used in the first PCR was C64U-R (5′-CGATTGTAGGAGACAATTGG-3′). For construction of pCB-C64U, pBaMV-C64U was cut with *Mfe*I and *Bam*HI and the fragment was ligated into a *Bam*HI/*Mfe*I digested pCB vector.

Construction of the 5′ end cDNA clones of natural BaMV isolates

For analysis of the 5′ sequences and secondary structures of natural BaMV variants, an ~500-bp cDNA fragments were amplified from the BaMV RNAs by the primer pair B82 [5′-GAAGGCCTGAAAAG(C)CAT(C)TCCAAAC A(G)-3′] and B165 (5′-CGGGAGGCGGGGGTAG ATAG-3′) using a RT-PCR kit (GE Healthcare, Buckinghamshire, UK). The amplified cDNA fragments were further cloned in a pGEM T-easy vector (Promega, WI, USA). All of the BaMV constructs were verified by DNA sequencing.

Synthesis of RNA transcripts *in vitro*

Plasmids were linearized by restriction enzyme. RNA transcripts with a 5′ cap structure (m7GpppG) were synthesized *in vitro* with T7 RNA polymerase as previously described (49).

Virus purification and viral RNA extraction

One-month-old *N. benthamiana* plants were inoculated with pCB, an infectious cDNA clone of BaMV-S (33). Nearly 7–10 days after infection, infected leaves were ground using a mortar and pestle, and crude sap was used for a second round of inoculation. Virions were purified from BaMV-S-infected leaves and viral RNA was extracted as described previously (53,54).

Protoplast inoculation and northern blot analyses

Preparation and RNA inoculation of protoplasts from *N. benthamiana* were as previously described (53). For each inoculation, protoplasts of 2×10^5 cells were inoculated with 1 µg of BaMV-S RNA alone or co-inoculated with different doses of satBaMV transcripts by electroporation (53). Total RNA extraction, glyoxalation, and northern blot analyses were carried out as previously described (49). For northern blot analyses, BaMV RNA and satBaMV RNA were probed with ^{32}P-labeled RNA probes specific for BaMV 3′ end (55) and full-length satBaMV, respectively (49). The hybridized membranes were washed by buffer and exposed on X-ray film (Kodak). Isotope intensity was processed and quantified by ImageQuant program (GE Healthcare, Buckinghamshire, UK).

Protoplast isolation and transfection

For direct DNA uptake experiments, protoplasts were isolated from 30-day-old *N. benthamiana* leaves as previously described (27). For each inoculation, different micrograms of plasmids were co-inoculated into 4×10^5 protoplasts by mixing with polyethylene glycol solution and incubated at 25°C. Thirty-six hours after transfection, protoplasts were harvested for northern blot analyses (49).

Plant inoculation

For mix-infection analyses, five leaves of 2-month-old *Chenopodium quinoa* plants were inoculated with 0.3 µg of BaMV-S RNA alone or co-inoculated with 0.3 µg of satBaMV transcripts. Local lesions generated on *C. quinoa* were counted at 7-day post-inoculation (dpi) and leaves were harvested for photography and Northern blot analysis. For mutational analyses, *C. quinoa* plants were inoculated with 0.5 µg of pCB or pCB-C64U alone or co-inoculated with 0.5 µg of pCBSF4 and pCBSL6. Leaves were harvested for photography and Northern blot analysis at 10 dpi.

RT-PCR and sequencing

The full-length satBaMV progenies were amplified by reverse transcription followed by PCR reaction. The conserved primer BS-43 [5′-GTCGAC**TCTAGA**T(15)-3′] (*Xba*I site is underlined) hybridized to the 3′-UTR of satBaMV was used for reverse transcription and primer BS-19 (5′-TGC**CTGCAG***TAATACGACTCACTATA*GA AAACTCACCGCAACGA-3′) (*Pst*I is underlined and the italic sequence represents the T7 promoter) hybridized to the 5′-UTR of satBaMV was added for PCR reaction. The resulting RT-PCR products were column-purified (Viogene, Taipei, Taiwan) and the amplified cDNA fragments were cloned in pGEM T-easy vector and used for DNA sequencing.

RESULTS

Interfering satBaMV is dominant in the mix-infection with non-interfering in *N. benthamiana* protoplasts

Satellite RNAs associated with BaMV in the natural field include interfering and non-interfering isolates, and several interfering satBaMVs have been identified, e.g. BSL6, BB23, DL11, DL16 and DL19 (17,46,47). To mimic the potentially mixed infection of satBaMV isolates that occur in BaMV infected plants in the field, *N. benthamiana* protoplasts were co-inoculated with a mixture of 1 µg of BaMV-S RNA and 0.5 µg each of BSF4 (non-interfering isolate) and BSL6 satBaMV transcripts alone or together. As shown in Figure 2B, inoculation with a mixture of equal amounts of BSL6 and BSF4 greatly diminished helper RNA accumulation in these two mixed populations of satBaMV RNAs in a manner similar to those inoculated with BSL6 alone at 24-h post-inoculation (hpi). To further identify the progeny of satBaMV, full-length cDNAs of satBaMV were amplified from the total RNA of co-inoculated protoplasts by RT-PCR. Sequence analyses of satBaMVs revealed that
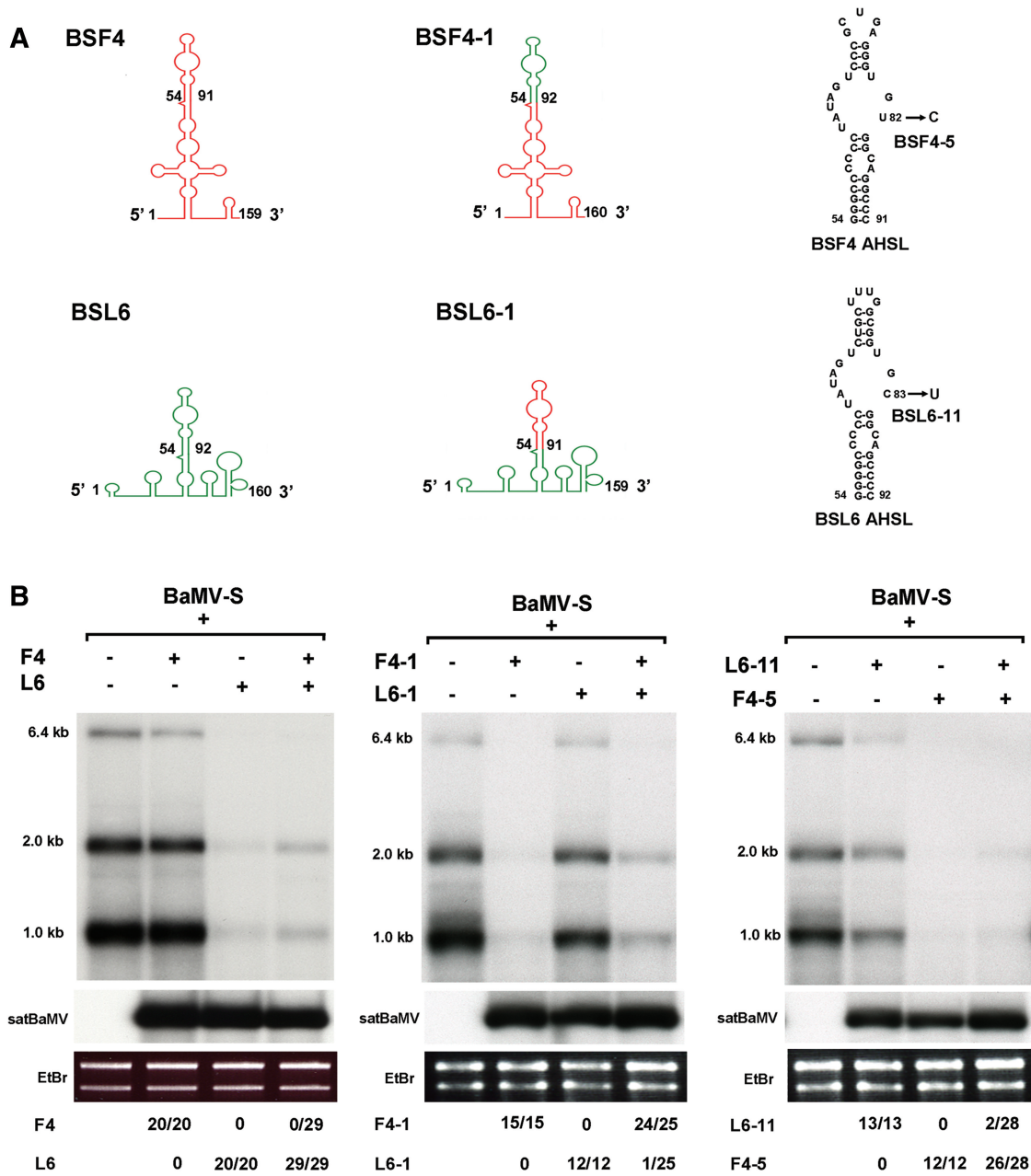
Figure 2. Identification of progeny satBaMV in *N. benthamiana* protoplasts co-infected with various satBaMVs. (**A**) Schematic representation of the secondary structure of 5′-UTR of BSF4 (green), BSL6 (red), and two satBaMV mutants, BSF4-1 and BSL6-1, in which the entire AHSLs were interchanged between BSF4 and BSL6. Sequences and AHSL structures of BSF4 and BSL6 and their derived mutants, BSF4-5 and BSL6-11 were shown. (**B**) The BaMV and satBaMV transcripts for inoculation are indicated above each lane. Lane '−': no satBaMV RNA added. Lane '+': satBaMV RNA was added as indicated. At 24-h post-inoculation (hpi), total RNAs isolated from 3×10^4 protoplasts were glyoxylated, electrophoresed in a 1% agarose gel, and transferred to a nylon membrane. Blots were hybridized with ^{32}P-labeled BaMV- (top) or satBaMV-specific probes (below). Positions of the BaMV genomic RNA (6.4 kb), 2.0 and 1.0 kb subgenomic RNA, and satRNA are indicated at the left. EtBr: ethidium bromide staining of the gel prior to the blotting shows approximately equal loading as revealed by ribosomal RNA abundance in each lane. The numbers of cloned cDNA of progeny satBaMV are indicated in the bottom panel.

29 of 29 cDNAs derived from progenies of mixed infection were BSL6 (Figure 2B), indicating the dominance of BSL6 in the progeny population. The BSL6 is also the dominant species of the satBaMV progeny population when mix-infected with another non-interfering isolate satBaMV-BV17 (data not shown). These data suggest that the replication competence of BSL6 is higher than that of BaMV and non-interfering satBaMVs.

To test whether this event is host-dependent, we also inoculated both of the satRNAs with BaMV RNA onto *C. quinoa* and observed the formation of local lesions. As expected, three repeated experiments showed that mix-infection of BSF4 and BSL6 markedly reduced the lesion formation on *C. quinoa* to ~15% compared to BaMV inoculation alone (data not shown). These results demonstrate that BSL6 is the dominant species of the

satBaMV progeny population in mix-infected protoplasts and plants.

A single nucleotide within the AHSL of BSL6 is crucial for dominance in mixed infection

We previously showed that the interchange of the AHSL between BSF4 and BSL6 alters the ability of satBaMV to interfere BaMV RNA accumulation (47). To further examine whether the modified interfering satBaMV (BSF4-1) is more competent than the non-interfering satBaMV mutant (BSL6-1) and BaMV during replication, BSF4-1 and BSL6-1 were used to perform an *in vivo* competition assay. BSF4-1 was derived from BSF4 with the AHSL replaced by that of BSL6, and BSL6-1 was modified from BSL6 with the AHSL replaced by that of BSF4 (Figure 2A). As shown in Figure 3B, BSF4-1 diminished the accumulation of helper RNA to ∼2% of that when inoculated with BaMV alone. Inoculation with a mixture of equal amounts of BSF4-1 and BSL6-1 greatly reduced BaMV RNA accumulation to ∼10% of that when inoculated with the helper virus alone. Full-length cDNA of RT-PCR followed by sequence analysis of satBaMV further revealed that 24 of 25 cDNAs derived from progenies of BSF4-1 and BSL6-1 mixed infection were BSF4-1, indicating the stable propagation and dominance of interfering BSF4-1 in the progeny population (Figure 2B).

A single-nucleotide change in the internal loop I (IL-I) of AHSL is sufficient to alter the biological activities of satBaMV (17). To further examine whether this change could compete for the RdRp complex, we investigated the replication competence of BSF4-5 and BSL6-11. BSF4-5 was derived from BSF4 with U^{82} replaced by C^{82} in the IL-I, and BSL6-11 was modified from BSL6 with C^{83} replaced by U^{83} (17). We found that BSF4-5 and mixed-infection of BSF4-5 and BSL6-11 greatly diminished the accumulation of helper RNAs to ∼2% and 7%, respectively, of that with BaMV alone. Of 28 cDNAs derived from progenies of BSF4-5 and BSL6-11 mixed infection, 26 were BSF4-5, indicating the dominance of BSF4-5 in the progeny population (Figure 2B).

These data suggest that the modified interfering sat BaMVs, even those with a single-nucleotide-substitution, compete for the replication machinery better than BaMV and non-interfering satBaMVs.

Replication efficiency of BSL6 is higher than that of BSF4

Recently, it was shown that over-expression of BaMV ORF1 was able to support satBaMV replication in *N. benthamiana* protoplasts, whereas the GDD motif (amino acids crucial for RdRp activity) deletion mutant of ORF1 did not (52). Thus, we set up an ORF 1-dependent system to support satBaMV replication. As shown in Figure 3A, under the support of BaMV replicase (pBaORF1), BSL6 is the dominant species of the satBaMV progeny population in pCBSF4 and pCBSL6 mix-infected protoplasts (Figure 3B). Similarly, 15 of 20 satBaMV progeny was pCBSF4-1 when mix-infected with pCBSL6-1, suggesting that the AHSLs of satBaMV play
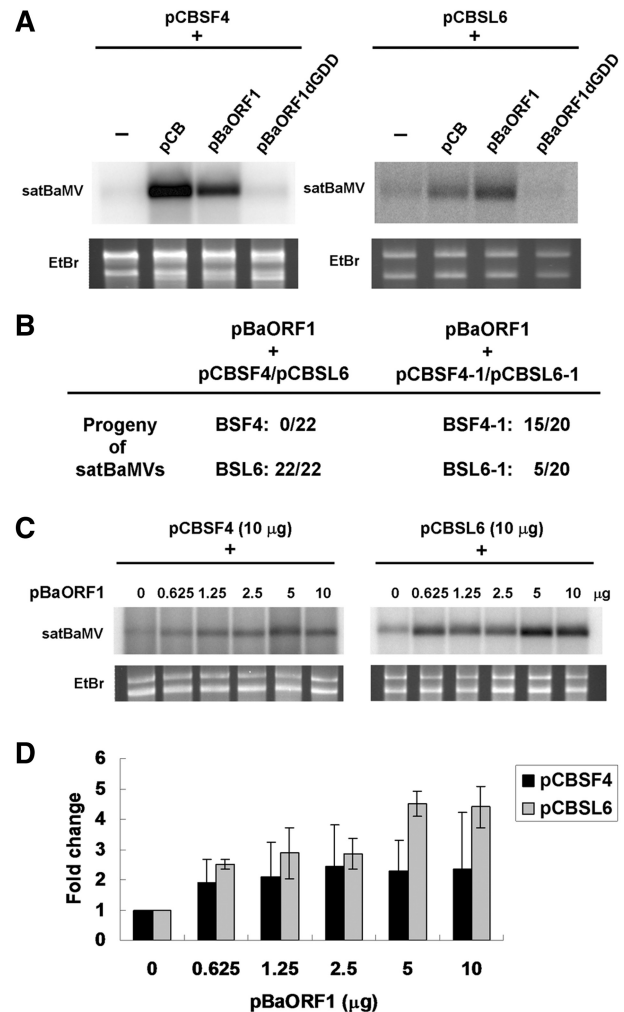

Figure 3. The replication efficiency of BSL6 was higher than that of BSF4 under the support of BaMV replicase in *N. benthamiana* protoplasts. (**A**) Northern blot analyses of satBaMV replication under the help of BaMV or BaMV replicase in protoplasts of *N. benthamiana*. The plasmids used for transfection were shown in the upper panel. Plasmids pCB, pCBSF4 and pCBSL6 were the infectious cDNA clones of BaMV-S, BSF4 and BSL6, respectively. Plasmids pBaORF1 and pBaORF1dGDD were the expression clones of wild-type and GDD motif deletion mutant of BaMV ORF1, respectively. (**B**) The numbers of cloned cDNA of progeny satBaMV in mix-infected population. (**C**) The accumulation levels of satBaMV RNAs under the support of different dose replicase in *N. benthamiana* protoplasts. (**D**) The bar chart shows the relative accumulation fold change of satBaMV RNAs in different doses of BaMV replicase. The input satRNA level in the absence of replicase was set as 1. The data are the average of three independent experiments.

a crucial role in competition for replicase in a BaMV-free system (Figure 3B). It also ruled out the possibility of RNA-RNA interaction between BaMV and satBaMV involved in BSL6 satBaMV-mediated interference of BaMV replication.

Since BSL6 is the dominant species of the satBaMV among progeny population of mix-infected protoplasts and plants, we further analyzed the replication efficiency of BSF4 and BSL6 by BaMV replicase in *N. benthamiana* protoplasts. As shown in Figure 3C and D, the accumulation levels of both BSF4 and BSL6 RNAs were

progressively elevated by increasing doses of BaMV replicase. Apparently, the increasing folds of BSL6 RNA were higher than those of BSF4 (Figure 3D). These results indicated that replication efficiency of BSL6 is higher than that of BSF4.

All natural BaMV isolates contain the conserved AHSL structures

Since the 5′ end of BaMV-S also contains an AHSL structure similar to that of satBaMV (Figure 4A) (17,18), we further analyzed the 5′ secondary structures of other natural BaMV isolates. As shown in Figure 4B, all 33 natural BaMV isolates sequenced contained the conserved AHSL structures regardless of whether they harbored satellite RNA or not. These results imply a co-evolution of the 5′ conserved AHSL structures in BaMV and satBaMV. Interestingly, all of the BaMV variants also contained the same critical $^{84}UGC^{86}$ in the IL-I and C^{64} in the IL-II as was found in interfering BSL6. The nucleotides at the equivalent positions of non-interfering satBaMV BSF4 and BSL4 were $^{80}UGU^{82}$ (BSF4) and U^{60} (BSL4), respectively (Figure 4A).

C^{64} and C^{86} in the AHSL contributes to BaMV replication efficiently

Similar to satBaMV, the AHSL also plays a crucial role in BaMV replication. Disrupting the structure or changing the loop sequences of AHSL affects the accumulation of BaMV-S RNAs (18). Since C^{60} and C^{83} in the internal loops of AHSL were crucial for downregulation of BaMV replication by BSL6 satBaMV (17), we wondered about the role of the conserved C^{64} and C^{86} of AHSL in BaMV replication. When *N. benthamiana* protoplasts were inoculated with the BaMV-C86U mutant, caused the accumulation of viral RNA was undetectable by Northern blot analysis at 24 hpi (Figure 5). Similarly, no symptoms or viral RNA could be found at 10 dpi when *C. quinoa* plants were inoculated with the BaMV-C86U mutant (data not shown), indicating that the nucleotide C^{86} of BaMV was essential for replication. However, replacing C^{64} with U reduced the replication efficiency of BaMV in both *N. benthamiana* protoplasts and *C. quinoa* plants to 20 and 46%, respectively (Figures 5 and 6). These results suggested that, similar to findings in satBaMV, C^{64} and C^{86} in the AHSL are also crucial to BaMV replication.
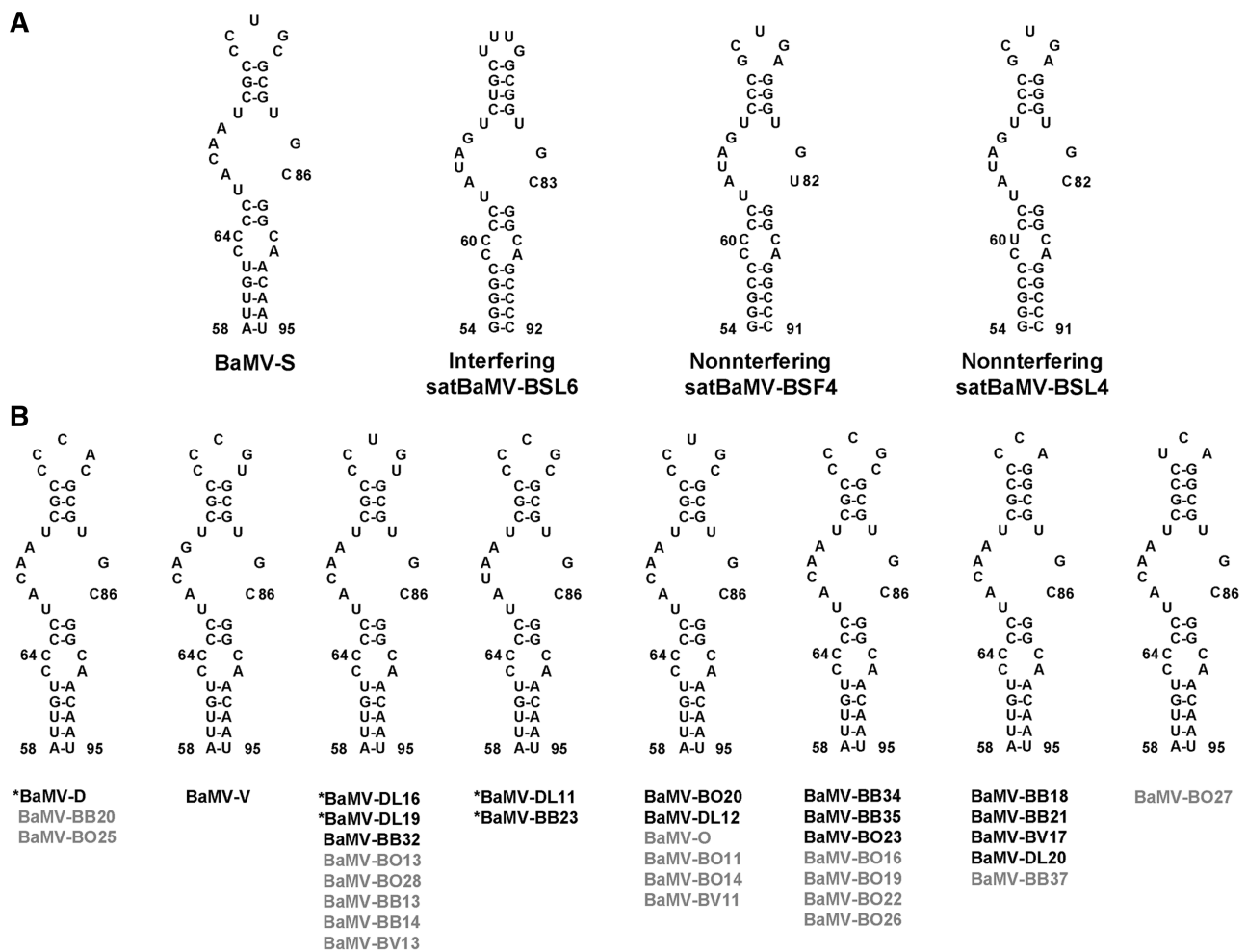

Figure 4. The predicted AHSL structures of natural BaMV isolates. (**A**) The 5′ conserved AHSL structures of BaMV-S and satBaMV variants. (**B**) The secondary structures of BaMV 5′ ends were predicted by Mfold program (56). BaMV variants with or without satellite RNA are shown in black and gray, respectively. Asterisk represents BaMV variants containing interfering satBaMV.
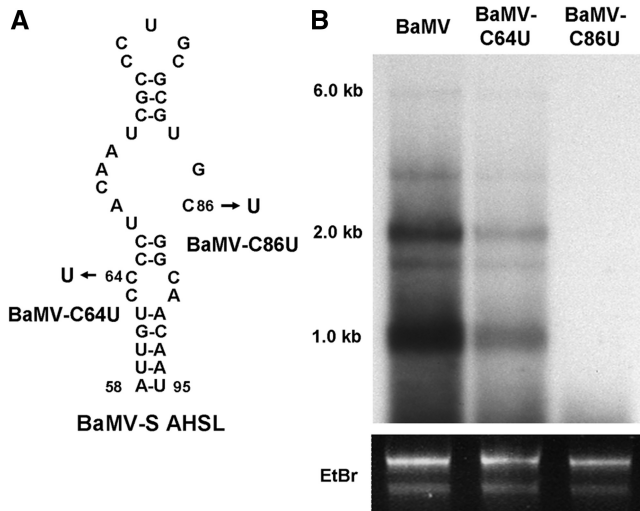
Figure 5. Specific nucleotides in the AHSL is involved in BaMV replication. (**A**) Sequences and AHSL structures of BaMV-S and its derived mutants, BaMV-C64U and BaMV-C86U. (**B**) Accumulation of BaMV RNAs in inoculated protoplasts at 24 hpi by northern blotting as described in Figure 2.

BSF4 satBaMV interferes with the replication of BaMV-C64U

The 5′ end of the BaMV-C64U mutant contains the AHSL with sequence and structure similar to that of non-interfering satBaMV. To evaluate the replication competence of BaMV-C64U and non-interfering satBaMV, *C. quinoa* plants were inoculated with pCB, the infectious clone of BaMV-S (33), or pCB-C64U alone or combined with the infectious clones of satBaMV (pCBSF4 or pCBSL6). Table 1 summarizes the local lesion production from three independent experiments. The pCB alone induced production with an average of about 173 lesions per leaf, while the lesions induced by pCB-C64U were at a level of 70% of those produced by pCB. The presence of BSL6 satBaMV resulted in great reduction of local lesion formation to a level of 7.5 and 8.3% of those produced by pCB and pCB-C64U, respectively (Table 1). Co-inoculation with BSF4 satBaMV slightly reduced the lesion number to 75% of that by pCB alone. However, the presence of BSF4 satBaMV significantly reduced the formation of local lesions to a level of 18.2% of those produced by pCB-C64U. Similar results were also found in another non-interfering satBaMV (satBaMV-BV17) (data not shown), indicating that non-interfering satBaMV could downregulate BaMV-C64U replication. Northern blot analyses revealed that BSL6, but not BSF4, greatly suppressed the accumulation of both BaMV-S genomic RNA and 1.0-kb subgenomic RNA in inoculated leaves at 10 dpi, whereas both BSF4 and BSL6 significantly decreased the accumulation level of BaMV-C64U RNAs (Figure 6B). Moreover, the accumulation level of BSF4 RNAs was significantly higher than that of BSL6 with the help of BaMV-C64U (Figure 6). This may be due to a greater reduction of BaMV by BSL6 compared to that
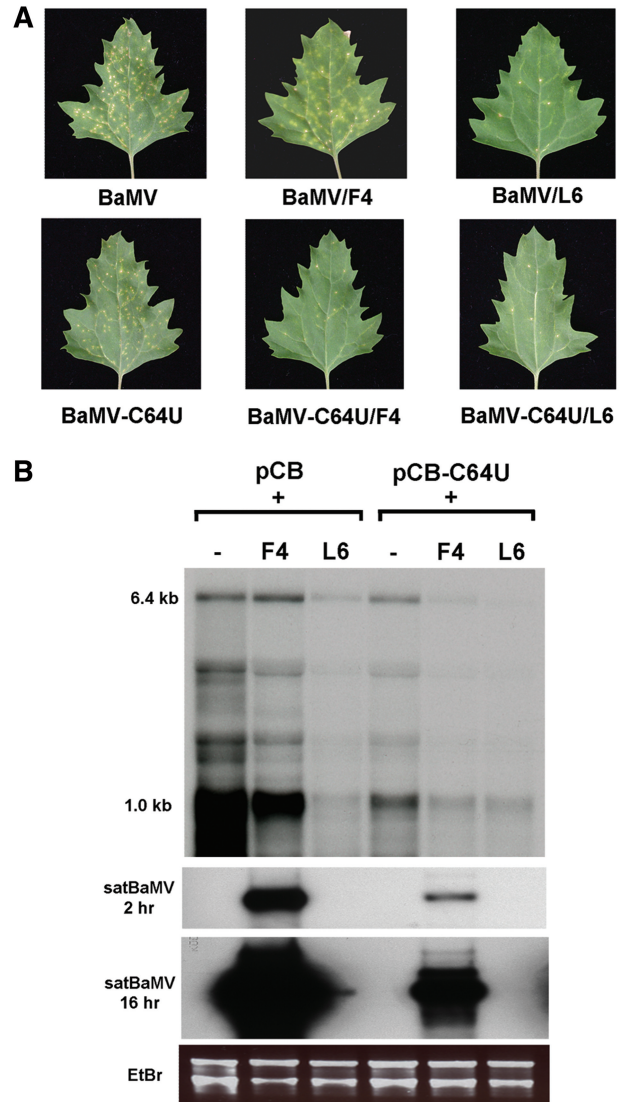

Figure 6. Non-interfering satBaMV interferes with the replication of the BaMV-C64U mutant. (**A**) Local lesions on *C. quinoa* leaves inoculated with pCB or pCB-C64U alone or co-inoculated with pCBSF4 or pCBSL6 at 10 dpi. (**B**) Northern blot of total RNA extracted from plants inoculated with infectious clones of BaMV and satBaMV at 10 dpi and hybridized with a probe specific to detect BaMV and satBaMV RNA. The different exposure times of films are indicated. To detect satBaMV BSL6 RNAs, the film was processed for 16 h.

by BSF4, and thus the replication of BSL6 was sequentially affected.

SatBaMV-mediated downregulation of BaMV replication is dose-dependent

We have routinely shown that BSL6 interferes with BaMV replication when the same weight (1 μg) of BaMV and satBaMV RNAs is used for co-inoculation in *N. benthamiana* protoplasts (46). Since the molar ratio of satBaMV/BaMV is 8:1 on an equal weight basis, we examined whether BSL6 could interfere with BaMV replication at low molar ratios. *Nicotiana benthamiana*

Table 1. Production of local lesions in *C. quinoa* co-inoculated with infectious clones of BaMV and satBaMV variants

	Average no. of local lesions/leaf[a]			
Inocula[b]	Experiment 1	Experiment 2	Experiment 3	Average (%)
pCB	90 ± 32	281 ± 23	147 ± 13	173 (100)
pCB/pCBSF4	77 ± 8	220 ± 15	93 ± 24	130 (75)
pCB/pCBSL6	8 ± 1	22 ± 3	8 ± 2	13 (7.5)
pCB-C64U	65 ± 11	206 ± 36	93 ± 11	121 (69.9)
pCB-C64U/ pCBSF4	24 ± 2	28 ± 2	13 ± 1	22 (12.7)
pCB-C64U/ pCBSL6	11 ± 4	13 ± 1	5 ± 1	10 (5.8)

[a]Each inoculum was inoculated onto three leaves of each plant. Data present the average numbers ± SEs of lesions per leaf from three inoculated plants and [b]For inoculum, 0.5 μg of pCB or pCB-C64U was used alone or mixed with 0.5 μg of pCBSF4 or pCBSL6.
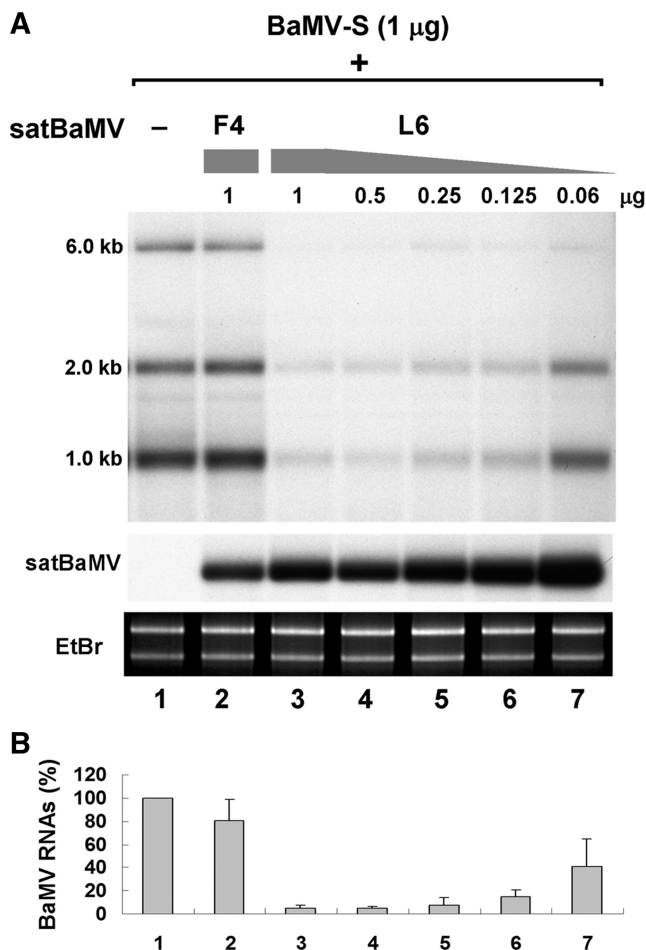

Figure 7. Dose-dependent interference with BaMV replication by satellite RNA. (**A**) Northern blot analyses of the accumulation of BaMV and satBaMV RNAs in *N. benthamiana* protoplasts inoculated with 1 μg of BaMV-S RNA alone or co-inoculated with 1 μg of BSF4 or different doses of BSL6 satBaMV transcripts. Northern blot analyses of the accumulation of BaMV and satBaMV RNAs in *N. benthamiana* protoplasts as described in Figure 2. (**B**) The bar chart shows the relative accumulation of BaMV RNAs in different molar ratios of satBaMV/BaMV. The data are the average of three independent experiments.

protoplasts were co-inoculated with a combination of 1 μg of BaMV-S RNA and different doses (1, 0.5, 0.25, 0.125 and 0.0625 μg) of BSL6 satBaMV transcripts. This converts the input molar ratios of satBaMV/BaMV to 8, 4, 2, 1 and 0.5, respectively. As shown in Figure 7, the accumulation level of BaMV RNAs was increased when the input molar ratio of satBaMV/BaMV was decreased (Figure 7, lanes 3–7). When the input molar ratio of satBaMV/BaMV was progressively reduced to 0.5, the level of BaMV RNAs was progressively increased to 41% of that of BaMV alone (Figure 7, lane 7). Interestingly, the accumulation level of BSL6 RNA was increased when the input molar ratio of satBaMV/BaMV was decreased (Figure 7A).

In summary, satBaMV-mediated interference with BaMV replication is dose-dependent, suggesting that this downregulation event may be due to competition with the helper virus for access to the replication machinery.

DISCUSSION

We previously showed that the sequence and structure of satBaMV 5′ AHSL are crucial for interference of BaMV replication (17,47,48). In this study, we demonstrate that both BaMV and satBaMV contain the conserved 5′ AHSL structures and sequences that are involved in replication competence, but that the particular nucleotides evolved in the AHSL for the efficient replication of BaMV are more constrained than those in satBaMV. Moreover, the interference of satBaMV in the downregulation of BaMV replication in the infected *N. benthamiana* protoplasts is dose-dependent, suggesting that satBaMV interference with BaMV replication may be due to their competition for access to limited replication machinery.

Interfering satBaMV with a conserved AHSL and specific C[83] is more competent than the non-interfering variant during replication

The error-prone replication of RNA replicons results in the quasispecies nature of RNA viruses and satellite RNAs in the natural field. Although satBaMVs have evolved into interfering and non-interfering species in the natural field (17,46,47), BaMV supported both interfering (BSL6) and non-interfering satBaMV (BSF4) replication equally in *N. benthamiana* protoplasts. In our competition assay in *N. benthamiana* protoplasts, a mixed population of BSF4 and BSL6 interfered with BaMV replication, and BSL6 was the sole dominant among progeny satBaMVs (Figure 2). Similar results were also found in BaMV-free satBaMV replication system (Figure 3B). Moreover, the replication rate of BSL6 was higher than that of BSF4 by the help of BaMV replicase alone (Figure 3C and D). These are strong lines of evidence suggesting that BSL6 outcompetes with BaMV and other satBaMVs for the replication machinery. Further analysis showed that the structure and specific nucleotides (C[64] and C[83]) of the AHSL, which are involved in interference with BaMV replication, are also required for replication competition among satBaMV variants (Figure 2B). Since a single nucleotide substitution

changes the phenotype of satBaMV (17), the existence of interfering species could easily result from the error-prone replication in the satBaMV RNA genome. Once an interfering species is generated in the satBaMV population, the interfering species would become the domain species after a number of replication cycles. In the case of CMV satRNAs, tomato plants co-inoculated with CMV and mixtures of non-necrogenic and necrogenic satRNA variants showed necrosis symptoms and the selective dominant accumulation of necrogenic satRNAs (24). This suggests that the necrosis domain of CMV satRNAs is also required for replication competition among satRNA variants. However, analyses of natural populations of CMV-satRNA revealed that the decrease of necrosis in the field was due to the evolution of the populations toward decreased virulence (57). The necrosis symptoms caused the death of host plants and consequently affected the replication of CMV and satRNA. In our study, analyses of 20 individual cDNA clones from another natural interfering satBaMV-DL11 population revealed that all were interfering species (N. S. Lin and H. C. Chen, unpublished data). However, the interfering species was only 10% in the non-interfering satBaMV-BV17 population (N. S. Lin and H. C. Chen, unpublished data). This could be due to the quasispecies dynamic nature of satBaMV, i.e. the interfering species might be a newly adapted one in the satBaMV population present at the time of sample collection, or may have been influenced by unknown factors such as a helper virus or other changes in the host and environment. Since interfering satBaMVs are also highly dependent on helper viruses for replication, over time the fitness of each RNA species in a population with a relatively depleted BaMV helper will be modulated. SatBaMVs will redefine their adaptation in response to the composition of population changes. This is why a majority of the satBaMVs we isolated from the natural population are non-interfering species (17,45–47).

Conserved AHSLs in the 5′ ends of BaMV and satBaMV

As a parasite of BaMV, satBaMV has evolved a 5′ AHSL structure similar to that of BaMV but with a relaxed degree of constrain for replication. Two major AHSL structures, conserved and less conserved, are present in the 5′-UTRs of natural satBaMV isolates (45). Most of satBaMV isolates maintain the conserved AHSL structure, a result of the co-variation of nucleotide substitutions in the HV region (45). In contrast, the nucleotide sequences of the AHSL in our BaMV isolates were much conserved and no co-variation was found in the stems of the AHSL, suggesting a purified selection (Figure 4). It is possible that the formation of the bottom stem of the BaMV 5′ AHSL requires 2 nt in the ORF1 start codon (Figure 1B), which is essential for the translation of RdRp.

A comparison of the sequences of the AHSLs of BaMV and satBaMV shows that the greatest divergence is located at the apical loop and in the base pairs within the bottom stem. It is worth noting that the structure and the nucleotides of the AHSLs in BaMV and satBaMV required for their replication were not totally the same. SatBaMV can tolerate sequence variations on the apical loop of the AHSL, whereas BaMV cannot (17,18). The change of cytosine (C^{83}) to U in the IL-I of the AHSL causes a loss in interfering ability but does not affect the replication ability in satBaMV (17). However, mutation at the equivalent position ($C^{86} \rightarrow U$) of the BaMV 5′ AHSL diminishes replication (Figure 5). Moreover, replacing the upper cytosine (C^{64}) with U in the IL-II of the AHSL reduces the replication efficiency of BaMV-C64U (Figures 5 and 6), whereas no affect on satBaMV replication was observed when the same mutation was introduced (17). Although non-interfering satBaMV could compete with the low replicating BaMV mutant (BaMV-C64U) (Figure 6), the C64U and C86U mutants were not found in natural BaMV isolates (Figure 4), suggesting a restriction of nucleotide change imposed by the AHSL formation. It has been shown that a single C-to-U substitution in loop B of the stem loop IV of an *enterovirus* internal ribosome entry site greatly changes the shape and flexibility of RNA (58). In the present study, a single C-to-U substitution in the AHSLs of BaMV and satBaMV did not change the secondary structure, but may possibly have altered the tertiary structure of the AHSL. It is also likely that the nucleotides changed at the equivalent positions of BaMV and satBaMV AHSLs differ in their effects on the AHSL structures. The differential requirements for nucleotides in the AHSL of BaMV and satBaMV suggest that other sequences or structures in their genomes are also involved in the stability of the AHSL structure. Whether the AHSL like 5′ termini of other RNA viruses can bind the viral and/or host factors to facilitate genome synthesis (59), or recruit to the replication site on the membranes (60,61) remains to be further investigated. However, we have excluded the potential long-range RNA-RNA interactions between BaMV and satBaMV by BaMV-free satBaMV replication system. The roles of AHSL structures in BaMV and satBaMV replication still need to be explored.

Satellite RNA-mediated downregulation of BaMV replication is dose-dependent

Previously, the reduction of CMV replication by satRNA was shown to compete with the helper virus for replication by way of the RdRp complex (62). Moreover, the symptom expression patterns in tomato plants infected with CMV-77.2 and the mixture of Tfn- and 77-satRNA are dependent on the ratio of two satRNA variants (24). Our results also show that the level of BSL6's interference with BaMV replication depends on the molar ratio of satBaMV/BaMV, and that the accumulation level of BSL6 RNA is inversely proportional to the inoculated satBaMV/BaMV ratio (Figure 7). Based on their genome size and a ratio of BaMV/satBaMV of 8:1, the rate of minus-strand satBaMV RNA synthesis is 8-fold faster than that of BaMV. Thus, the progeny of BSL6 could compete for more replication factors and downregulate BaMV replication even when the molar ratio of BaMV/satBaMV was reduced to 1 in co-inoculated *N. benthamiana* protoplasts (Figure 7). However, more

RdRp was translated from increasing levels of BaMV when the molar ratio of satBaMV/BaMV was decreased below 1. Subsequently, more satBaMV RNAs were amplified at the early stage of co-infection (e.g. 24 hpi). After 24 hpi, the high accumulation level of BSL6 RNA may likely continue to downregulate BaMV replication.

ACKNOWLEDGEMENTS

FUNDING

REFERENCES

1. Mandahar,C.L. (2006) Multiplication of RNA plant viruses. *Springer*, 10–14.
2. Buck,K.W. (1996) Comparison of the replication of positive-stranded RNA viruses of plants and animals. *Adv. Virus Res.*, **47**, 159–251.
3. Liu,Y., Wimmer,E. and Paul,A.V. (2009) Cis-acting RNA elements in human and animal plus-strand RNA viruses. *Biochim. Biophys. Acta*, **1789**, 495–517.
4. Miller,W.A., Wang,Z. and Treder,K. (2007) The amazing diversity of cap-independent translation elements in the 3′-untranslated regions of plant viral RNAs. *Biochem. Soc. Trans.*, **35**, 1629–1633.
5. Lough,T.J., Lee,R.H., Emerson,S.J., Forster,R.L. and Lucas,W.J. (2006) Functional analysis of the 5′ untranslated region of potexvirus RNA reveals a role in viral replication and cell-to-cell movement. *Virology*, **351**, 455–465.
6. Damayanti,T.A., Tsukaguchi,S., Mise,K. and Okuno,T. (2003) cis-acting elements required for efficient packaging of brome mosaic virus RNA3 in barley protoplasts. *J. Virol.*, **77**, 9979–9986.
7. Qu,F. and Morris,T.J. (1997) Encapsidation of turnip crinkle virus is defined by a specific packaging signal and RNA size. *J. Virol.*, **71**, 1428–1435.
8. Sleat,D.E., Turner,P.C., Finch,J.T., Butler,P.J. and Wilson,T.M. (1986) Packaging of recombinant RNA molecules into pseudovirus particles directed by the origin-of-assembly sequence from tobacco mosaic virus RNA. *Virology*, **155**, 299–308.
9. Hu,C.C., Hsu,Y.H. and Lin,N.S. (2009) Satellite RNAs and satellite viruses of plants. *Viruses*, **1**, 1325–1130.
10. Roossinck,M.J., Sleat,D. and Palukaitis,P. (1992) Satellite RNAs of plant viruses: structures and biological effects. *Microbiol. Rev.*, **56**, 265–279.
11. Simon,A.E., Roossinck,M.J. and Havelda,Z. (2004) Plant virus satellite and defective interfering RNAs: new paradigms for a new century. *Annu. Rev. Phytopathol.*, **42**, 415–437.
12. Huang,Y.W., Hu,C.C., Lin,N.S. and Hsu,Y.H. (2010) Mimicry of molecular pretenders: the terminal structures of satellites associated with plant RNA viruses. *RNA Biol.*, **7**, 162–171.
13. Stupina,V. and Simon,A.E. (1997) Analysis in vivo of turnip crinkle virus satellite RNA C variants with mutations in the 3′-terminal minus-strand promoter. *Virology*, **238**, 470–477.
14. Ray,D., Na,H. and White,K.A. (2004) Structural properties of a multifunctional T-shaped RNA domain that mediate efficient tomato bushy stunt virus RNA replication. *J. Virol.*, **78**, 10490–10500.
15. Wu,B., Vanti,W.B. and White,K.A. (2001) An RNA domain within the 5′ untranslated region of the tomato bushy stunt virus genome modulates viral RNA replication. *J. Mol. Biol.*, **305**, 741–756.
16. Gordon,K.H. and Symons,R.H. (1983) Satellite RNA of cucumber mosaic virus forms a secondary structure with partial 3′-terminal homology to genomal RNAs. *Nucleic Acids Res.*, **11**, 947–960.
17. Chen,H.C., Hsu,Y.H. and Lin,N.S. (2007) Downregulation of Bamboo mosaic virus replication requires the 5′ apical hairpin stem loop structure and sequence of satellite RNA. *Virology*, **365**, 271–284.
18. Chen,S.C., Desprez,A. and Olsthoorn,R.C. (2010) Structural homology between bamboo mosaic virus and its satellite RNAs in the 5′ untranslated region. *J. Gen. Virol.*, **91**, 782–787.
19. Huang,Y.W., Hu,C.C., Lin,C.A., Liu,Y.P., Tsai,C.H., Lin,N.S. and Hsu,Y.H. (2009) Structural and functional analyses of the 3′ untranslated region of Bamboo mosaic virus satellite RNA. *Virology*, **386**, 139–153.
20. Domingo,E. and Holland,J.J. (1994) The Evolutionary Biology of Viruses. In: Morse,S.S. (ed.), Raven Press, New York, pp. 161–184.
21. Garcia-Arenal,F. and Palukaitis,P. (1999) Structure and functional relationships of satellite RNAs of cucumber mosaic virus. *Curr. Top. Microbiol. Immunol.*, **239**, 37–63.
22. Taliansky,M.E. and Robinson,D.J. (1997) Down-regulation of groundnut rosette virus replication by a variant satellite RNA. *Virology*, **230**, 228–235.
23. Taliansky,M.E., Ryabov,E.V., Robinson,D.J. and Palukaitis,P. (1998) Tomato cell death mediated by complementary plant viral satellite RNA sequences. *Mol. Plant Microbe Interact.*, **11**, 1214–1222.
24. Cillo,F., Finetti-Sialer,M.M., Papanice,M.A. and Gallitelli,D. (2004) Analysis of mechanisms involved in the Cucumber mosaic virus satellite RNA-mediated transgenic resistance in tomato plants. *Mol. Plant Microbe Interact.*, **17**, 98–108.
25. Celix,A., Rodriguez-Cerezo,E. and Garcia-Arenal,F. (1997) New satellite RNAs, but no DI RNAs, are found in natural populations of tomato bushy stunt tombusvirus. *Virology*, **239**, 277–284.
26. Lin,N.S., Lin,B.Y., Lo,N.W., Hu,C.C., Chow,T.Y. and Hsu,Y.H. (1994) Nucleotide sequence of the genomic RNA of bamboo mosaic potexvirus. *J. Gen. Virol.*, **75(Pt 9)**, 2513–2518.
27. Yang,C.C., Liu,J.S., Lin,C.P. and Lin,N.S. (1997) Nucleotide sequence and phylogenetic analysis of a bamboo mosaic potexvirus isolate from common bamboo (Bambusa vulgaris McClure). *Bot. Bull. Acad. Sin.*, **38**, 77–84.
28. Huang,Y.L., Han,Y.T., Chang,Y.T., Hsu,Y.H. and Meng,M. (2004) Critical residues for GTP methylation and formation of the covalent m7GMP-enzyme intermediate in the capping enzyme domain of bamboo mosaic virus. *J. Virol.*, **78**, 1271–1280.
29. Huang,Y.L., Hsu,Y.H., Han,Y.T. and Meng,M. (2005) mRNA guanylation catalyzed by the S-adenosylmethionine-dependent guanylyltransferase of bamboo mosaic virus. *J. Biol. Chem.*, **280**, 13153–13162.
30. Li,Y.I., Chen,Y.J., Hsu,Y.H. and Meng,M. (2001) Characterization of the AdoMet-dependent guanylyltransferase activity that is associated with the N terminus of bamboo mosaic virus replicase. *J. Virol.*, **75**, 782–788.
31. Li,Y.I., Shih,T.W., Hsu,Y.H., Han,Y.T., Huang,Y.L. and Meng,M. (2001) The helicase-like domain of plant potexvirus replicase participates in formation of RNA 5′ cap structure by exhibiting RNA 5′-triphosphatase activity. *J. Virol.*, **75**, 12114–12120.

32. Li,Y.I., Cheng,Y.M., Huang,Y.L., Tsai,C.H., Hsu,Y.H. and Meng,M. (1998) Identification and characterization of the Escherichia coli-expressed RNA-dependent RNA polymerase of bamboo mosaic virus. *J. Virol.*, **72**, 10093–10099.

33. Lin,M.K., Chang,B.Y., Liao,J.T., Lin,N.S. and Hsu,Y.H. (2004) Arg-16 and Arg-21 in the N-terminal region of the triple-gene-block protein 1 of Bamboo mosaic virus are essential for virus movement. *J. Gen. Virol.*, **85**, 251–259.

34. Wung,C.H., Hsu,Y.H., Liou,D.Y., Huang,W.C., Lin,N.S. and Chang,B.Y. (1999) Identification of the RNA-binding sites of the triple gene block protein 1 of bamboo mosaic potexvirus. *J. Gen. Virol.*, **80(Pt 5)**, 1119–1126.

35. Lan,P., Yeh,W.B., Tsai,C.W. and Lin,N.S. (2010) A unique glycine-rich motif at the N-terminal region of Bamboo mosaic virus coat protein is required for symptom expression. *Mol. Plant Microbe Interact.*, **23**, 903–914.

36. Lin,N.S. and Hsu,Y.H. (1994) A satellite RNA associated with bamboo mosaic potexvirus. *Virology*, **202**, 707–714.

37. Chen,I.H., Lin,J.W., Chen,Y.J., Wang,Z.C., Liang,L.F., Meng,M., Hsu,Y.H. and Tsai,C.H. (2010) The 3′-terminal sequence of Bamboo mosaic virus minus-strand RNA interacts with RNA-dependent RNA polymerase and initiates plus-strand RNA synthesis. *Mol. Plant Pathol.*, **11**, 203–212.

38. Bancroft,J.B., Rouleau,M., Johnston,R., Prins,L. and Mackie,G.A. (1991) The entire nucleotide sequence of foxtail mosaic virus RNA. *J. Gen. Virol.*, **72(Pt 9)**, 2173–2181.

39. White,K.A., Bancroft,J.B. and Mackie,G.A. (1992) Mutagenesis of a hexanucleotide sequence conserved in potexvirus RNAs. *Virology*, **189**, 817–820.

40. Cheng,C.P. and Tsai,C.H. (1999) Structural and functional analysis of the 3′ untranslated region of bamboo mosaic potexvirus genomic RNA. *J. Mol. Biol.*, **288**, 555–565.

41. Tsai,C.H., Cheng,C.P., Peng,C.W., Lin,B.Y., Lin,N.S. and Hsu,Y.H. (1999) Sufficient length of a poly(A) tail for the formation of a potential pseudoknot is required for efficient replication of bamboo mosaic potexvirus RNA. *J. Virol.*, **73**, 2703–2709.

42. Chen,I.H., Meng,M., Hsu,Y.H. and Tsai,C.H. (2003) Functional analysis of the cloverleaf-like structure in the 3′ untranslated region of bamboo mosaic potexvirus RNA revealed dual roles in viral RNA replication and long distance movement. *Virology*, **315**, 415–424.

43. Huang,C.Y., Huang,Y.L., Meng,M., Hsu,Y.H. and Tsai,C.H. (2001) Sequences at the 3′ untranslated region of bamboo mosaic potexvirus RNA interact with the viral RNA-dependent RNA polymerase. *J. Virol.*, **75**, 2818–2824.

44. Liu,J.S., Hsu,Y.H., Huang,T.Y. and Lin,N.S. (1997) Molecular evolution and phylogeny of satellite RNA associated with bamboo mosaic potexvirus. *J. Mol. Evol.*, **44**, 207–213.

45. Yeh,W.B., Hsu,Y.H., Chen,H.C. and Lin,N.S. (2004) A conserved secondary structure in the hypervariable region at the 5′ end of Bamboo mosaic virus satellite RNA is functionally interchangeable. *Virology*, **330**, 105–115.

46. Hsu,Y.H., Lee,Y.S., Liu,J.S. and Lin,N.S. (1998) Differential interactions of bamboo mosaic potexvirus satellite RNAs, helper virus, and host plants. *Mol. Plant Microbe Interact.*, **11**, 1207–1213.

47. Hsu,Y.H., Chen,H.C., Cheng,J., Annamali,P., Lin,B.Y., Wu,C.T., Yeh,W.B. and Lin,N.S. (2006) Crucial role of the 5′ conserved structure of bamboo mosaic virus satellite RNA in downregulation of helper viral RNA replication. *J. Virol.*, **80**, 2566–2574.

48. Annamalai,P., Hsu,Y.H., Liu,Y.P., Tsai,C.H. and Lin,N.S. (2003) Structural and mutational analyses of cis-acting sequences in the 5′-untranslated region of satellite RNA of bamboo mosaic potexvirus. *Virology*, **311**, 229–239.

49. Lin,N.S., Lee,Y.S., Lin,B.Y., Lee,C.W. and Hsu,Y.H. (1996) The open reading frame of bamboo mosaic potexvirus satellite RNA is not essential for its replication and can be replaced with a bacterial gene. *Proc. Natl Acad. Sci. USA*, **93**, 3138–3142.

50. Chang,B.Y., Lin,N.S., Liou,D.Y., Chen,J.P., Liou,G.G. and Hsu,Y.H. (1997) Subcellular localization of the 28 kDa protein of the triple-gene-block of bamboo mosaic potexvirus. *J. Gen. Virol.*, **78(Pt 5)**, 1175–1179.

51. Lin,M.K., Hu,C.C., Lin,N.S., Chang,B.Y. and Hsu,Y.H. (2006) Movement of potexviruses requires species-specific interactions among the cognate triple gene block proteins, as revealed by a trans-complementation assay based on the bamboo mosaic virus satellite RNA-mediated expression system. *J. Gen. Virol.*, **87**, 1357–1367.

52. Prasanth,K.R., Huang,Y.W., Liou,M.R., Wang,R.Y., Hu,C.C., Tsai,C.H., Meng,M., Lin,N.S. and Hsu,Y.H. (2011) Glyceraldehyde 3-phosphate dehydrogenase negatively regulates the replication of Bamboo mosaic virus and its associated satellite RNA. *J. Virol.*, **85**, 8829–8840.

53. Lin,N.S., Huang,T.Z. and Hsu,Y.H. (1992) Infection of barely protoplasts with bamboo mosaic virus RNA. *Bot. Bull. Acad. Sin.*, **33**, 271–275.

54. Lin,N.S. and Chen,C.C. (1991) Association of Bamboo mosaic virus (BaMV) and BaMV-specific electron-dense crystalline bodies with chloroplasts. *Phytopathology*, **81**, 1551–1555.

55. Lin,K.Y., Cheng,C.P., Chang,B.C., Wang,W.C., Huang,Y.W., Lee,Y.S., Huang,H.D., Hsu,Y.H. and Lin,N.S. (2010) Global analyses of small interfering RNAs derived from Bamboo mosaic virus and its associated satellite RNAs in different plants. *PLoS One*, **5**, e11928.

56. Zuker,M. (2003) Mfold web server for nucleic acid folding and hybridization prediction. *Nucleic Acids Res.*, **31**, 3406–3415.

57. Escriu,F., Fraile,A. and Garcia-Arenal,F. (2000) Evolution of virulence in natural populations of the satellite RNA of cucumber mosaic virus. *Phytopathology*, **90**, 480–485.

58. Du,Z., Ulyanov,N.B., Yu,J., Andino,R. and James,T.L. (2004) NMR structures of loop B RNAs from the stem-loop IV domain of the enterovirus internal ribosome entry site: a single C to U substitution drastically changes the shape and flexibility of RNA. *Biochemistry*, **43**, 5757–5771.

59. Andino,R., Rieckhof,G.E. and Baltimore,D. (1990) A functional ribonucleoprotein complex forms around the 5′ end of poliovirus RNA. *Cell*, **63**, 369–380.

60. Chen,J., Noueiry,A. and Ahlquist,P. (2001) Brome mosaic virus Protein 1a recruits viral RNA2 to RNA replication through a 5′ proximal RNA2 signal. *J. Virol.*, **75**, 3207–3219.

61. Pogany,J., White,K.A. and Nagy,P.D. (2005) Specific binding of tombusvirus replication protein p33 to an internal replication element in the viral RNA is essential for replication. *J. Virol.*, **79**, 4859–4869.

62. Wu,G. and Kaper,J.M. (1995) Competition of viral and satellite RNAs of cucumber mosaic virus for replication in vitro by viral RNA-dependent RNA polymerase. *Res. Virol.*, **146**, 61–67.